Chapter 17

# NON-DECAYING CURRENTS IN NORMAL METALS

I. O. Kulik
*Department of Physics, Bilkent University*
*06533 Bilkent, Ankara, Turkey*

**Abstract** In a present paper, we review cases when stable, time-independent currents may flow in normal metals, both single-connected or multiple-connected, in presence of magnetic field or the field of vector potential. These include the spatially oscillating currents in narrow metallic stripes originating due to Landau diamagnetism (the Landau persistent currents), the currents in hollow normal-metal or semiconducting cylinders and rings induced by the Aharonov-Bohm flux threading the conducting loop (the Aharonov-Bohm persistent currents), and currents in hollow cylinders subject to radial flux and existing even in the absence of the longitudinal, or Aharonov-Bohm flux (the "transverse" persistent currents), as well as the non-decaying currents in axial magnetic field, modulated via the Berry phase effect by the transverse or azimuthal components of the field and oscillating as a function of the latter.

## 1. INTRODUCTION

It is commonly believed that current in a normal (nonsuperconducting) metal can only flow if the voltage is applied to the sample, and that current transport is necessarily related to the Joule heat dissipation inside the sample. This is however a prejudice. To start with, the diamagnetic properties of metals (the Landau diamagnetism) can be explained by currents flowing around the sample near its surface, as was first demonstrated by Teller [1] in his interpretation of the Landau theory [2]. The other case is the Aharonov-Bohm effect [3] in double connected metallic samples which produces currents created by the magnetic flux inside the sample orifice. It was long debated, especially by Byers and Yang [4] and by Bloch [5] whether stable currents may exist in the noninteract-



*I. O. Kulik and R. Ellialtioğlu (eds.),*
*Quantum Mesoscopic Phenomena and Mesoscopic Devices in Microelectronics*, 259–282.

ing electron gas without the off-diagonal long range order specific to superconductivity. Bloch, in particular, concluded that

"Except for abnormally small radius and irrespective of the specific properties of the system one is thus led to the exclusion of stable flux trapping in a one dimensional ring".

The "small radius" corresponds to what we call now mesoscopic sample. In the latter, stable current and flux trapping is possible. It was first clearly stated by the author [6] that the non-decaying current DOES exist in a small metallic loop provided that scattering of electrons (both elastic and inelastic) is not too strong. In the paper [6] it was concluded that

"The current state corresponds in this case to a minimum of the free energy, so that allowance for dissipation does not lead to its decay".

Later, Buttiker, Imry and Landauer [7] reached the same conclusion by considering Aharonov-Bohm current in a dirty ring, showing that the magnetic flux $\Phi$ in a ring serves as a quasi-momentum if the ring is unwrapped into an effective periodic structure with a period equal to the ring circumference $L$. Therefore, the energy becomes a periodic function of $\Phi$ with a period of a normal-metal flux quantum $\Phi_0 = hc/e$, and the current originates as a nonzero derivative $J = -c\,\partial E/\partial\Phi$.

The purpose of the present paper is to review and extend the situations in which non-decaying ("persistent") current may exist in non-superconducting metals. The cases considered include the spatially oscillating currents in narrow metallic stripes in a magnetic field responsible for the Landau diamagnetism (the Landau persistent currents), the currents driven by the Aharonov-Bohm flux in hollow metallic cylinders and rings (the Aharonov-Bohm persistent currents), and the non-decaying charge flow in hollow disordered cylinders subject to radial magnetic flux (the "transverse" persistent currents), as well as the non-decaying currents originating due to Berry's phase [8] effects for electron spins interacting with the radial and azimuthal magnetic fields in the ring. Part of the material presented can also be found in the review papers related to the Aharonov-Bohm effect in solids [9]-[15], *etc.*

## 2. PERSISTENT CURRENT IN A LONG METALLIC STRIPE

Consider a situation when magnetic field $\mathbf{B}$ is applied perpendicular to the surface of two-dimensional metallic stripe with electron density $n$ and width $d$ (Fig. 17.1). The sample will show the Landau effect; *i.e.*, the dependence of its energy $E$ on $B$ and thus attaining the magnetic moment $M_z = -\partial E/\partial B$. We will assume that the width of the stripe

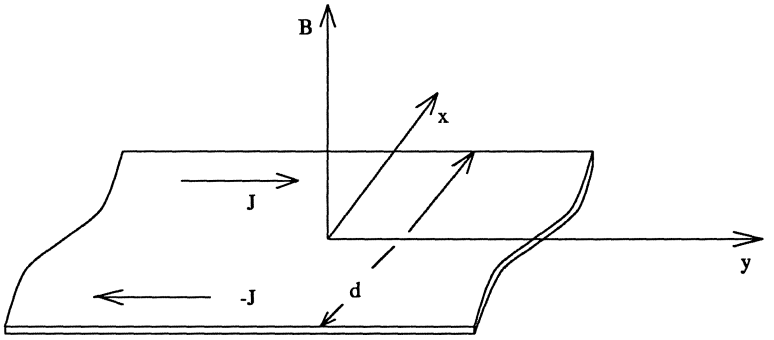


*Figure 17.1* Sketch of a two-dimensional metallic stripe of width $d$ in a perpendicular magnetic field **B**. Arrows show the average current direction in the stripe.

$d$ is much smaller than the cyclotron radius $r_H = mv_F c/eB$ which will allow to include the effect of magnetic field as a perturbation, and to find the current density from the Schrödinger equation expanded in powers of $B$. Neglecting the spin, Schrödinger equation reads

$$-\frac{\hbar^2}{2m}\frac{\partial^2\psi}{\partial x^2} - \frac{\hbar^2}{2m}\left(\frac{\partial}{\partial y} - \frac{ieBx}{\hbar c}\right)^2 \psi = E\psi. \tag{17.1}$$

In zero magnetic field, the eigenstates of Eq. 17.1 are

$$\psi^0_{nk} = \frac{1}{\sqrt{L}} e^{iky} \left(\frac{2}{d}\right)^{1/2} \sin\frac{\pi n}{d}(x + d/2) \tag{17.2}$$

corresponding to energies

$$\varepsilon^0_n = \frac{\hbar^2}{2m}\left(k^2 + \pi^2 n^2/d^2\right).$$

The perturbation Hamiltonian is

$$H_1 = \frac{\hbar^2}{2m}\left(2kk_0\frac{x}{d} + k_0^2\frac{x^2}{d^2}\right) \tag{17.3}$$

where $k_0 = eBd/\hbar c$. To first order in $B$, it has matrix elements

$$(H_1)_{mn} = \frac{2kk_0\hbar^2}{m}\int_0^1 \sin\pi n\left(\xi - \frac{1}{2}\right)\sin\pi m\left(\xi - \frac{1}{2}\right)\xi d\xi =$$

$$= \begin{cases} -\frac{8\hbar^2 kk_0}{\pi^2 m}\frac{nm}{(n^2-m^2)^2} & \text{if } n-m \text{ is odd} \\ 0 & \text{otherwise} \end{cases} \tag{17.4}$$

It is then a straightforward to solve for the correction to the wave function and to the current. The current density is

$$j(\xi) = -j_0 \sum_{n=1}^{\infty} \int_{-\infty}^{\infty} \frac{d\kappa}{e^{(\kappa^2+n^2-n_F^2)/2n_F\tau}+1}$$

$$\times \left[ \left(\xi - \frac{1}{2}\right) \sin^2 \pi n\xi - \frac{32\kappa^2}{\pi^2} \sum_{m=1}^{\infty} \frac{nm\delta_{n-m,2k+1}}{(n^2-m^2)^3} \sin \pi n\xi \sin \pi m\xi \right] \quad (17.5)$$

where $\xi = x/d$, $j_0 = 2e\hbar k_0/md^2 = 2e^2B/mcd$, and $\tau = T/\Delta E$ where $\Delta E = hp_F/md$ is the distance between discrete energy levels in a ring at the Fermi energy. The dependence $j(\xi)$ is calculated numerically and shown in Fig. 17.2 at various temperatures $T$.

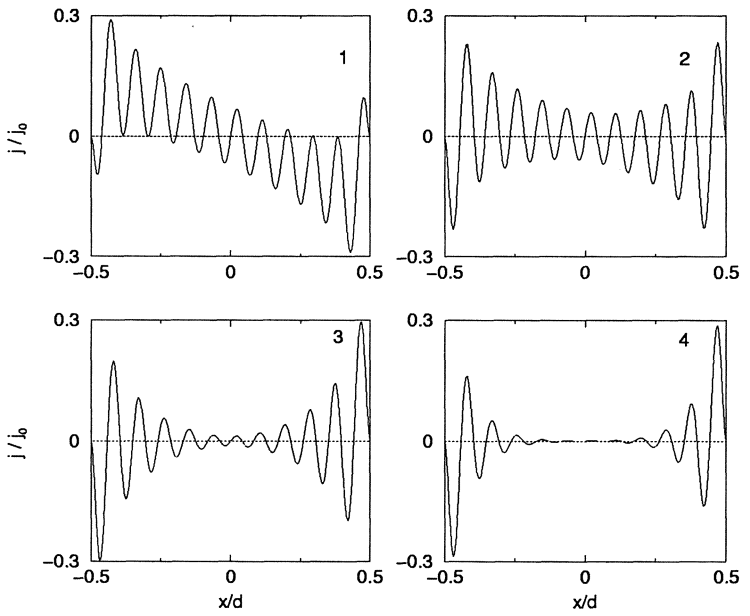


*Figure 17.2* Persistent current in a stripe at various temperatures. Panel 1: $\tau = 0$; panel 2: $\tau = 0.15$; panel 3: $\tau = 0.45$; panel 4: $\tau = 0.9$ where $\tau$ is the temperature in units of the level spacing $\Delta E$ at the Fermi energy $\varepsilon_F$. The value of the electron concentration corresponds to the "Fermi number" $n_F$ defined according to $\varepsilon_F = h^2 n_F^2/2md^2$ and equal to $n_F = 10.9$.

First of all, our calculation shows that the current does exist. Since it corresponds to minimum of free energy (at given magnetic field) it does not decay in time, even if the scattering is included to the calculation. Integration of the current $j(\xi)$ with a factor $(\xi - 1/2)$ gives magnetic

moment $M$ of the sample which in our case (in thin sample) proves to be temperature dependent, unlike in the standard Landau diamagnetism in bulk samples.

The current will not vanish (but may decrease in amplitude) if scattering is included, in the same way as the Landau diamagnetism persists in dirty metals. This argument does not show need for any further justification of the persistent current. (We can find proof even on the experimental basis, referring to the innumerable papers studying the manifestations of the Landau diamagnetism, the De Haas - Van Alphen effect [16].)

The current in a stripe shows periodic oscillation at low temperature with a spatial period

$$\lambda = \frac{2\pi}{Q_0}, \quad Q_0 = 2k_F \tag{17.6}$$

where $k_F$ is the Fermi momentum. These oscillations is nothing else than the known Friedel oscillation in a degenerate Fermi liquid [17]. At elevated temperature, the amplitude of oscillation decreases in the middle of the sample, and current is pushed to the specimen edges. Mention that the amplitude of oscillation is much greater than the average current. At higher temperature, amplitude of oscillation follows the exponential law with a characteristic decay length

$$\xi_T = \frac{\hbar v_F}{2\pi T} \tag{17.7}$$

which reveals also in such phenomena as the Andreev reflection [18] from the normal metal backed to superconductor [19].

# 3. PERSISTENT CURRENTS IN METALLIC RINGS AND CYLINDERS

## 3.1 Clean Rings

In a one-dimensional metallic ring pierced by solenoid creating Aharonov-Bohm flux $\Phi = A_\varphi L$ where $A_\varphi$ is the vector potential and $L$ is the ring circumference (Fig. 17.3), the Schrödinger equation

$$\frac{-\hbar^2}{2mR^2}\left(\frac{\partial}{\partial\varphi} - \frac{ieAL}{hc}\right)^2 \psi = E\psi \tag{17.8}$$

has a solution

$$\psi_n = \frac{1}{\sqrt{L}} e^{in\varphi} \tag{17.9}$$

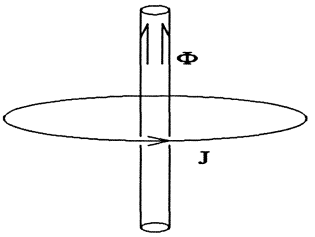


*Figure 17.3* One-dimensional metallic ring in the field of vector potential created by the solenoid piercing the ring.

corresponding to electron energy

$$\varepsilon_n = \frac{\hbar^2}{2mR^2}\left(n - \frac{\Phi}{\Phi_0}\right)^2 \tag{17.10}$$

where $\Phi_0 = hc/e$ is the flux quantum.

The thermal averaged current in a ring is calculated as

$$J = \frac{eh}{mL^2}\sum_{n=-\infty}^{\infty} \frac{n - \Phi/\Phi_0}{e^{\left[\left(n-\Phi/\Phi_0\right)^2 - n_F^2\right]/2n_F\tau} + 1} \tag{17.11}$$

where we introduced $\tau$ as a relative temperature $\tau = T/\Delta E$ where $\Delta E$ is the distance between two successive levels of the discrete spectrum (Eq. 17.10) at the energy equal to Fermi energy ($\varepsilon_F = h^2 n_F^2/2mL^2$)

$$\Delta E = h^2 n_F/mL^2 = hv_F/L. \tag{17.12}$$

Straightforward calculation using the Poisson formula

$$\sum_{n=-\infty}^{\infty} f(n) = \sum_{-\infty}^{\infty} \int_{-\infty}^{\infty} f(n) e^{2\pi i n s} dn$$

gives the current as an oscillating function of flux with the period $\Phi_0$

$$J = \frac{ev_F}{\pi L}\sum_{s=1}^{\infty} \frac{2\pi^2 s\tau}{\sinh(2\pi^2 s\tau)} \cos(k_F L s) \sin\left(2\pi s \frac{\Phi}{\Phi_0}\right). \tag{17.13}$$

At low temperature, amplitude of oscillation is of the order

$$J_{\max} \sim \frac{ev_F}{\pi L} \text{ at } T \to 0. \tag{17.14}$$

At higher temperature, only the lowest harmonic ($s = 1$) survives with an amplitude

$$J_{\max}^{1d} \simeq \frac{ev_F}{L}\frac{4\pi T}{\Delta E} e^{-2\pi^2 T/\Delta E}, \; T \geq \Delta E. \tag{17.15}$$

In a two-dimensional sample (thin hollow cylinder of radius $R$), persistent current is proportional to the number of transverse conducting channels [6]

$$J_{\max}^{2d} \simeq \frac{4\sqrt{2\pi}}{\sqrt{k_F L}} \frac{ev_F}{L} N_\perp \frac{4\pi T}{\Delta E} e^{-2\pi^2 T/\Delta E} \tag{17.16}$$

where $N_\perp = L_z k_F/2\pi$, whereas in the three-dimensional ring of cross section $S = d_1 d_2$ it increases with the number of perpendicular channels $N_\perp = k_F^2 S/4\pi$ as

$$J_{\max}^{3d} \sim \frac{ev_F}{L} N_\perp^{1/2}. \tag{17.17}$$

## 3.2 Ring Interrupted By A Barrier

Assume that one-dimensional ring is interrupted by a barrier $V\delta(x)$ where $x$ is a coordinate along the ring, $x = R\varphi$ such that $0 \le x \le L = 2\pi R$. The solution to the Schrödinger equation is of the form

$$\psi = C_1 e^{ik_1 x} + C_2 e^{-ik_2 x} \tag{17.18}$$

where $k_{1,2} = k \pm eA/\hbar c$ and $k = \sqrt{2m\varepsilon}/\hbar$, with $C_1$, $C_2$ found from the boundary condition

$$\psi(0) = \psi(L) \text{ and } -\frac{\hbar^2}{2m}[\psi'(0) - \psi'(L)] + V\psi(0) = 0. \tag{17.19}$$

The allowed energy values are found from the equation equivalent to the $1d$ Kronig-Penney model

$$\cos kL + \frac{mV}{\hbar^2 k} \sin kL = \cos 2\pi \frac{\Phi}{\Phi_0}. \tag{17.20}$$

The wave function (Eq. 17.18), with the constriction implied by this equation, can be rewritten in the form

$$\psi = Ce^{i\alpha \frac{x}{L}} \left( e^{-i\alpha/2} \sin \kappa \frac{x}{L} + e^{i\alpha/2} \sin \kappa \frac{L-x}{L} \right) \tag{17.21}$$

where

$$C = \frac{1}{\sqrt{L}} \left[ 1 + \frac{\sin \kappa}{\kappa} (\cos \kappa - \cos \alpha) - \cos \kappa \cos \alpha \right]^{-\frac{1}{2}}. \tag{17.22}$$

By introducing the dimensionless momentum $\kappa = |k|L$, Eq. (17.20) is rewritten as

$$\cos \kappa + g \frac{\sin \kappa}{\kappa} = \cos \alpha \tag{17.23}$$

where $g = mVL/\hbar^2$ and $\alpha = 2\pi\Phi/\Phi_0$. Persistent current in the ring is found as an average of the current operator $\hat{j} = \frac{e\hbar}{m}(\frac{1}{i}\frac{\partial}{\partial x} - \frac{eA}{\hbar c})$ and equals

$$j = -\frac{e\hbar}{mL}\sum_n \frac{\kappa_n \sin\kappa_n \sin\alpha}{1 + \frac{\sin\kappa_n}{\kappa_n}(\cos_n - \cos\alpha) - \cos\kappa_n \cos\alpha}. \tag{17.24}$$

In case of no barrier ($V = 0$), the solutions of Eq. (17.23) are $\kappa_n = 2\pi n + \alpha$, $n = 0, \pm 1, \pm 2, ...$ which of course bring us back to the previous formula (Eq. 17.10). In the opposite limit of a strong barrier, $g_o \gg 1$ (where $g_o = g/k_F L = mV/\hbar^2 k_F \sim Vk_F/\varepsilon_F$; $Vk_F$ is an effective barrier height of a potential with an effective width $\Delta x$ of the order of the Fermi wavelength $2\pi/k_F$) the solution to Eq. (17.23) is

$$\kappa_n \simeq \pi n + \frac{1}{g_o}\frac{(-1)^n \cos\alpha - 1}{k_F L}. \tag{17.25}$$

We receive in this limit the formula for the persistent current

$$J = J_{\max} \sin 2\pi \frac{\Phi}{\Phi_0} \tag{17.26}$$

with the maximal amplitude

$$J_{\max} \simeq \frac{ev_F}{L}\left(\frac{l}{L}\right)^{1/2} \sum_{n=1}^{\infty} \frac{(-1)^n n^2}{e^{(n^2 - n_F^2)/2n_F\tau} + 1} \tag{17.27}$$

In the latter expression, we introduced an effective mean free path of electron in the ring

$$l \simeq L\frac{D}{1-D} \tag{17.28}$$

where $D$ is the barrier transmissivity $D \sim 1/g_o^2$. It then follows from Eq. (17.27) that persistent current decreases with the transmissivity of the barrier slower than the normal-state conductance of the ring $G \sim (ne^2 S/p_F)(l/L)$ does.

## 3.3 Dirty Rings

Elastic scattering of electrons decreases the amplitude of persistent current oscillation. The impurities can be viewed as barriers which increase the effective length needed for electron to make a full round up of the ring and to interfere with the initial state. The interference between the initial and the final states showing the effect of the Aharonov-Bohm flux persists until the length becomes of the order of the localization

length $\zeta \sim lN_\perp$ in a bulk sample [20] where $N_\perp = k_F^2 S_\perp / 4\pi$ is the number of transverse channels in a ring of cross section $S_\perp$. In the diffusive regime,

$$l \ll L \ll \zeta, \tag{17.29}$$

conductance of the ring can be calculated as a scattering problem, by using the Landauer formula [21] (see also [10]) relating ring conductance $G$ to the transmission amplitudes $t_{\alpha\beta}$ between the incoming and outgoing channels $\alpha$ and $\beta$

$$G = \frac{2e^2}{h} \sum_{\alpha,\beta} |t_{\alpha\beta}|^2. \tag{17.30}$$

We therefore estimate the ring conductance as

$$G \sim N_\perp \langle |t|^2 \rangle G_0 \tag{17.31}$$

where $G_0 = 2e^2/h = 1/12.9\mathrm{k}\Omega$ is the quantum of conductance, *i.e.*, $G$ is proportional to square of transmission amplitude. The Aharonov-Bohm effect, on the contrary, is expected to relate amplitude of the persistent current *linearly* to $|t_{\alpha\beta}|$, as was shown above in case of model problem with a $\delta$-functional barrier. Translated from the subsection 2, the value of persistent current is expected to be, by the order of magnitude

$$J_{\max} \sim \frac{ev_F}{L} \left( \frac{G}{G_0} \right)^{1/2}. \tag{17.32}$$

We may expect that similar dependences may hold also for a diffusive ring. And indeed, the numeric simulation of the Aharonov-Bohm current in disordered ring seems to support this hypothesis.

In Fig. 17.4, we show the mean free path dependence of the current amplitude at zero temperature, which was received by calculating the energy $E$ of $N$ electrons in a $3d$ ring of volume $d_1 d_2 L$ with varying defect concentration, as function of vector potential $A$, and then calculating the current as a derivative $dE/dA$. Within the tight-binding approximation, the Hamiltonian of the model is

$$H = -t \sum_{\mathbf{n}} \sum_{\mathbf{m}} a^+_{\mathbf{n}+\mathbf{m}} a_{\mathbf{n}} e^{i\alpha m_x} + \sum_{\mathbf{n}} V_{\mathbf{n}} a^+_{\mathbf{n}} a_{\mathbf{n}} \tag{17.33}$$

where $\alpha = 2\pi\Phi/N\Phi_0$ is the phase difference between the near lattice sites along the ring circumference, $a^+_{\mathbf{n}}$ ($a_{\mathbf{n}}$) the creation (annihilation) operators at site $\mathbf{n}$, and $\mathbf{m}$ is the vector pointing from $\mathbf{n}$ to the nearest site. Potential at the site $V_{\mathbf{n}} = V\xi_{\mathbf{n}}$ is a random quantity depending on the value of $\xi_{\mathbf{n}} = 0, 1$ where 1 is occurring with a probability $c$. This probability determines the impurity concentration and the electron

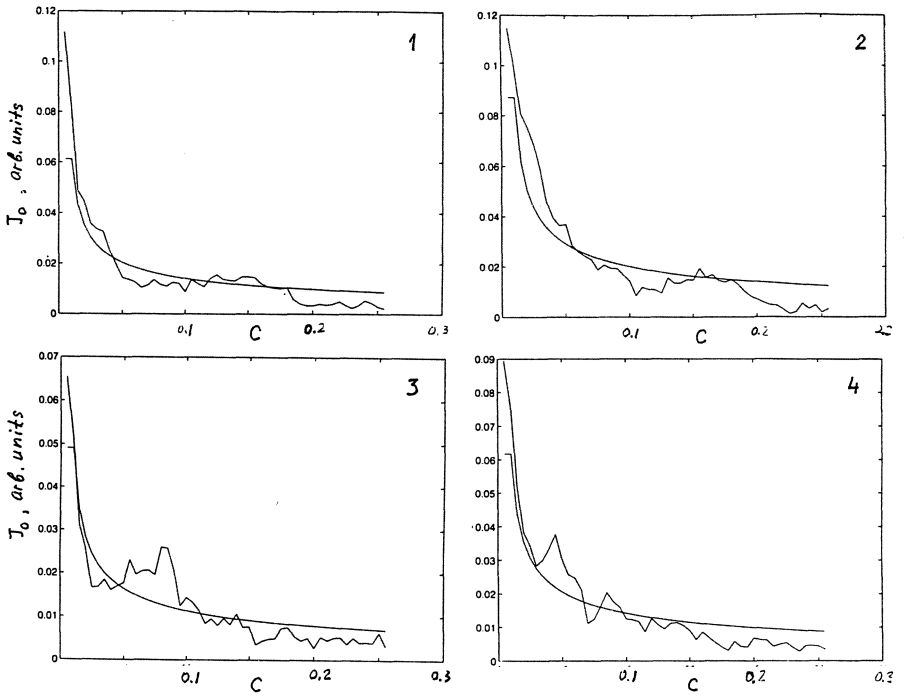


*Figure 17.4* Persistent current amplitude $J$ versus defect concentration $c$ in a disordered ring (zigzag line) compared to the empirical $J(c)$ dependence according to Eq. (17.31) (continuous line). The dependences have been received in the various runs of numeric experiment with different number of electrons $N_e$ and gradually increasing concentration $c$. Panel 1: $N_e = 25$; panel 2: $N_e = 35$; panel 3: $N_e = 45$; panel 4: $N_e = 50$. The sample has a cross section of $4 \times 4$ sites and a perimeter length of 30 sites. The "theoretical" curves have been received by estimating electron mean free path from the estimate $l \sim a/c$ where $a$ is intersite spacing) and fitting the magnitude of the current at smaller concentration used ($c = 0.05$) to the "experimental" value at that concentration.

mean free path $l \sim a/c$ ($a$ is the intersite distance taken as unity in our units). The limit $V \to \infty$ is equivalent to breaking of all connections of a site having $\xi_n = 0$ to its neighbors.

The irregular curves in Fig. 17.4 represent the change in the magnitude of persistent current at addition of new defect sites (thus increasing $c$ and decreasing $l$) whereas the smooth curves show the empirical law (17.32) with $G$ estimated from Eq. (17.31) and corrected to the value of conductance at $c = 0$. The above calculations are not fully convincing since the expected localization limit is almost equal to the ring length,

in our relatively small rings, and show disagreement with other theories [22] predicting smaller persistent currents. Mention however that some experimental data [23] in which persistent current, if have been properly estimated, was found to be *larger* than the value calculated on basis of Ref. [22]. Other experimental works [24, 25] show smaller oscillation amplitude.

## 3.4 Weak Localization Effects

Disordered metals show the effect of quantum interference in the Aharonov-Bohm field in an another way, as was first pointed out by Aronov, Altshuler and Spivak [26], and observed in an experiment of Sharvin and Sharvin [27]. The mesoscopic rings display oscillatory dependence of their kinetic rather than thermodynamic properties on the flux piercing the ring, with the half of the Aharonov-Bohm period, $hc/2e$. The origin of these oscillations is in that the time-reversed paths of electrons traversing the ring circumference in the clockwise and in the counterclockwise directions interfere with one another giving rise to conductance oscillations with the period equal to $\Phi_0/2$

$$\sigma \sim \sin\left(\frac{2e}{\hbar c}\oint \mathbf{A}dl\right) \sim \sin\left(4\pi\frac{\Phi}{\Phi_0}\right). \tag{17.34}$$

Extensive reviews on that subject are presented in Refs. [9, 11, 28].

# 4. FLUCTUATIONS OF PERSISTENT CURRENT

Persistent current is not a macroscopic phenomenon like, *e.g.*, supercurrent in a ring. The amplitude of persistent current in a $1d$ ring is of the order of the current produced by a *single* electron orbiting the ring with a *high* velocity, that of the order of the Fermi velocity $v_F \sim 10^8$ cm/s. This makes a current to be of a sizeable amplitude

$$J \sim 1\ \mu\text{A}$$

in a ring of radius $R \sim 10^{-4}$ cm. More than that, unlike the superconducting currents, persistent current in mesoscopic loop is subject to quantum and thermal fluctuations. The average current equals to

$$\langle \hat{J} \rangle = \sum_n \langle \hat{J} \rangle_n N_n \tag{17.35}$$

where $\hat{J}$ is the current operator and $N_n$ is the thermal average of the occupation probability of a quantum state $n$. The root mean square

(RMS) fluctuation of the current, $\langle \delta \hat{J}^2 \rangle^{1/2}$, is found from the identity

$$\delta \bar{J}^2 = \langle (\hat{J} - \langle \hat{J} \rangle)^2 \rangle = \sum_n \langle \hat{J}^2 \rangle_n N_n - \langle \hat{J} \rangle_n^2 N_n^2 \tag{17.36}$$

Consider a ring with a $\delta$-barrier from Section 3.2. The average value of the current density $j$ is given by Eq. (17.24), whereas the average value of $j^2$ is

$$\langle \hat{j^2} \rangle_n = \langle \hat{j} \rangle_n^2 = \left( \frac{e\hbar}{mL^2} \right) \kappa_n^2. \tag{17.37}$$

In a ballistic ring, we receive

$$\delta \hat{J}^2 = \left( \frac{ev_F}{L} \right)^2 \frac{1}{(4\pi n_F)^2} \sum_{n=-\infty}^{\infty} \frac{(n-f)^2}{\cosh^2 \frac{(n-f)^2 - n_F^2}{4\pi n_F}} \tag{17.38}$$

which gives

$$\langle \delta \hat{J}^2 \rangle \simeq \left( \frac{ev_F}{L} \right)^2 \frac{T/\Delta E}{2\pi k_F L}. \tag{17.39}$$

In a poorly connected ring ($V_{max} \gg \varepsilon_F$ where $V_{max} = Vk_F$ is an effective height of the barrier) the average value of the persistent current becomes smaller than the RMS fluctuations of the current. The motion of electrons is then more like the "persistent drift" rather than the regular flow of charge similar to that in a superconducting metal.

## 5. TRANSVERSE PERSISTENT CURRENT

Persistent current in ring appears due to violation of the time-reversal symmetry created by the "longitudinal" flux directed along the ring symmetry axis. The nonzero $\varphi$-component of vector potential, $A_\varphi$, determines the asymmetry between the clockwise and counterclockwise directions, and allows for the nonzero $\varphi$-component of the current. Assume however that in a double ring (Fig. 17.5*a*) the total longitudinal flux is zero but the radial flux (the one due to $B_r$ component of the field) is not. If the double-ring is asymmetric, the phase gradients in two rings will not be equal to one another which is equivalent to the appearance of an effective phase gradient in the $\varphi$-direction. The current in a system (termed in [29] as the "transverse" persistent current), may then appear even if the longitudinal flux is zero. The experimental observation of persistent currents in strong transverse magnetic fields was also reported in Ref. [30].

Assume that hopping amplitudes $t_1$, $t_2$ in a double ring are not equal, and that the hopping amplitude $t_{12}$ couples the rings. Such model, in a

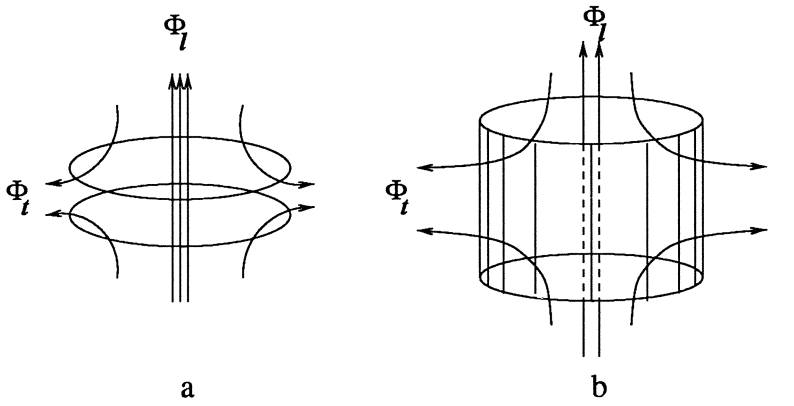


*Figure 17.5* Sketch of a setup for observation of the Aharonov-Bohm effect in a strong perpendicular field. (a) Two coupled rings; (b) Hollow cylinder with walls traversed by the transverse flux $\Phi_t$ created by magnetic field in the radial direction. Shown are lines of force of magnetic field around the cylinder.

tight-binding approximation, is described by the Hamiltonian

$$H = -\sum_{n=1}^{N} \left( t_1 a_n^+ a_{n+1} e^{i(\alpha+\beta)} + t_2 b^+ +_n b_{n+1} e^{i(\alpha-\beta)} + t_{12} a_n^+ b_n \right) + \text{H.c.} \tag{17.40}$$

in which $\alpha$ stands for the longitudinal and $\beta$ for the transverse flux

$$\alpha = 2\pi\Phi/N\Phi_0, \ \beta = \pi\Phi_r/N\Phi_0. \tag{17.41}$$

Solving for the plane wave state

$$\psi = \sum_{n=1}^{N} e^{ikn}(Aa_n^+ + Bb_n^+)|0\rangle$$

we receive the energy

$$\varepsilon_{k\sigma} = -t_1 \cos(k+\alpha+\beta) - t_2 \cos(k+\alpha-\beta)$$

$$+\sigma\sqrt{(t_1 \cos(k+\alpha+\beta) - t_2 \cos(k+\alpha-\beta)^2 + t_{12}^2} \tag{17.42}$$

and then calculate the current

$$J = -\frac{e}{N\hbar} \sum_k \sum_{\sigma=-1}^{1} \left[ e^{(\varepsilon_{k\sigma}-\zeta)/T} + 1 \right]^{-1} \frac{\partial}{\partial\alpha} \varepsilon_{k\sigma}(\alpha) \tag{17.43}$$

which may be nonzero even if the longitudinal flux $\Phi = 0$. Such "transverse" currents appear if system is not central symmetric, *e.g.*, when

$t_1 \neq t_2$. In a hollow dirty cylinder (Fig. 17.5*b*), asymmetry is caused by random distribution of impurities with the potential $V_{nm} = V\xi_{nm}$, $0 < \xi_{nm} < 1$

$$H = -t\sum_{n=1}^{N}\sum_{m=1}^{M}\left(a_{nm}^{+}a_{n+1,m}e^{i[\alpha+\beta(m-M/2)]} + a_{nm}^{+}a_{n,m+1}\right) + \text{H.c.} + \sum_{nm} V_{nm}a_{nm}^{+}a_{nm} \tag{17.44}$$

where $\alpha$ is given by first Eq. (17.41) and $\beta = 2\pi\Phi_r/NM$.

Fig. 17.6 shows an example of persistent current versus transverse flux dependence in a cylindrical shell with $10 \times 10$ sites and varying amplitude $V$ of the impurity potential. The chaotic quasi-oscillatory behavior is hard to interpret quantitatively, it corresponds most probably to the flux quantization in the local "loops" formed by the impurity islands. The dependence, if properly inverted, may serve as an information on the inhomogeneous state in mesoscopic structure.

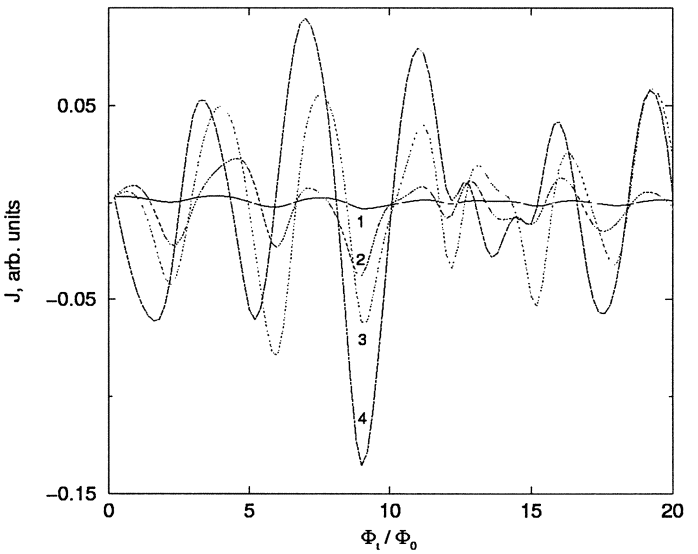


*Figure 17.6* Azimuthal current in a disordered cylindrical shell with $10 \times 10$ sites versus transverse flux through wall $\Phi_t$ at the zero Aharonov-Bohm flux $\Phi_l$ at various amplitudes of the disorder potential $V$. Line 1: $V/t = 0$; line 2: $V/t = 0.05$; line 3: $V/t = 0.1$; line 4: $V/t = 0.15$. The small but nonzero value of current at $V = 0$ is related to numeric procedure of calculating current as the derivative of energy with respect to flux and then putting flux $\Phi_l \to 0$.

# 6. BERRY'S PHASE AND OSCILLATORY SPIN DYNAMICS IN MESOSCOPIC RINGS

Aharonov-Bohm effect represents the first but not the last example of more general concept of quantal phase accumulated by electron in its motion in a slowly varying field which was considered by Berry [8] (see also [31]) in the context of molecular dynamics. When electron moves adiabatically (slower than the field changes) in the field of the vector potential, its wave function accumulates a phase

$$\Delta\varphi = \frac{e}{\hbar c}\int_{\mathbf{r}_1}^{\mathbf{r}_2} \mathbf{A}d\mathbf{l} = \frac{e}{\hbar c}A_\varphi(\theta_2 - \theta_1) \tag{17.45}$$

where $\theta_1$ and $\theta_2$ are azimuthal angles of the initial and final locations $\mathbf{r}_1$ and $\mathbf{r}_2$ on a ring. This phase difference is the Aharonov-Bohm phase discussed in previous sections. Consider now the effect of magnetic field on the electron spin. Assume that magnetic field at any point of the ring makes fixed orientation with the local tangential vector on the contour (Fig. 17.7). The tangential component of the field, $B_\varphi$, can in principle be created by a current-carrying wire inserted to the ring. The radial component, $B_r$, formally corresponds to the field produced by the line of magnetic monopoles inserted into the ring. In reality, such field can be created by a proper combination of solenoids around the ring, as was explained in Section 5 (see Fig. 17.6).

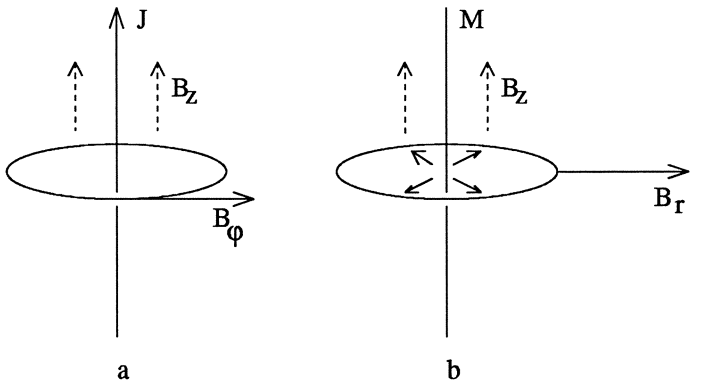


*Figure 17.7* Sketch of the thought Berry-phase experiments with an azimuthal field created by a current-carrying wire piercing the ring (a), and radial field generated by the line of magnetic monopoles inside the ring (b).

When electron is slowly rotating along the ring, its spin function will accumulate phase due to spinor transformation [32]

$$\exp\left[\frac{1}{2}i\mathbf{n}\cdot\vec{\sigma}(\theta_2 - \theta_1)\right]$$

where $\vec{\sigma}$ is the Pauli matrix vector and $\mathbf{n}$ is the unit vector along the rotation axis. With $\mathbf{n}$ being in the direction of the vector $\mathbf{B}$, this produces a phase difference between the points $\theta_1$, $\theta_2$ on the ring

$$\Delta\varphi = \frac{1}{2}(\theta_2 - \theta_1)\sin\alpha \tag{17.46}$$

where $\alpha$ is an angle between $\mathbf{B}$ and its projection onto the plane of the ring. Such effects which are additive to the topological effects of the Aharonov and Bohm, have been considered by Stern [33] and by Loss, Goldbart and Balatsky [34]. Actually, the condition for adiabaticity explains the origin of the effect rather is strictly required. The theory of the Berry's phase effects for electron spin, as well as the Aharonov-Bohm effects due to the orbital motion of electrons in a ring, will be presented below in a form which covers both the adiabatical ($\omega_H T_0 \gg 1$) as well as nonadiabatical ($\omega_H T_0 \leq 1$) regimes where $\omega_H$ is the cyclotron frequency $eB/mc$ and $T_0^{-1}$ the frequency of electron rotation $v_F/L$.

Hamiltonian of particle in a ring including the Zeeman energy in the nonrelativistic approximation (the Pauli Hamiltonian),

$$H = \frac{1}{2m}\left(\hat{\mathbf{p}} - \frac{e}{c}\mathbf{A}\right)^2 - \mu\mathbf{B}\cdot\vec{\sigma}, \tag{17.47}$$

is presented in a matrix form

$$H = -\varepsilon_0\left(\frac{\partial}{\partial\varphi} - i\Phi/\Phi_0\right)^2 + \varepsilon_\perp\begin{pmatrix} 0 & e^{-i(\varphi+\gamma)} \\ e^{i(\varphi+\gamma)} & 0 \end{pmatrix} + \varepsilon_{||}\begin{pmatrix} 1 & 0 \\ 0 & -1 \end{pmatrix} \tag{17.48}$$

where $\varepsilon_0$ is the ring quantization energy, and $\varepsilon_\perp$ and $\varepsilon_{||}$ are the components of the Zeeman energy $\varepsilon_Z = g\mu_B B$

$$\varepsilon_0 = \hbar^2/2mR^2, \quad \varepsilon_\perp = \varepsilon_Z\cos\alpha, \quad \varepsilon_{||} = \varepsilon_Z\sin\alpha. \tag{17.49}$$

$\gamma$ is the angle between the radial and azimuthal components of magnetic field $\gamma = \arctan(B_\varphi/B_r)$. $\Phi$ is the total flux comprising that from the $z$-component of magnetic field and from the solenoid which can in principle be inserted into the ring. Eigenstates of Eq. (17.48) can easily be found if we present the wave function in the form

$$\Psi = \sum_{n=-\infty}^{\infty}\begin{pmatrix} u_n \\ v_n \end{pmatrix} e^{in\varphi} \tag{17.50}$$

and write down the equations for $u_n$, $v_n$

$$\begin{aligned} \varepsilon_0(n - \Phi/\Phi_0)^2 u_n + \varepsilon_\perp e^{-i\gamma}v_{n+1} + \varepsilon_{||}u_n &= \varepsilon u_n, \\ \varepsilon_0(n - \Phi/\Phi_0)^2 v_n + \varepsilon_\perp e^{-i\gamma}u_{n-1} - \varepsilon_{||}v_n &= \varepsilon v_n. \end{aligned} \tag{17.51}$$

Then we receive an equation

$$\left[\varepsilon_0(n-f)^2+\varepsilon_{||}-\varepsilon+\frac{\varepsilon_\perp^2}{\varepsilon-\varepsilon_0(n+1-f)^2+\varepsilon_{||}}\right]u_n=0 \qquad (17.52)$$

where $f=\Phi/\Phi_0$, and the relation between $u_n$ and $v_{n+1}$

$$v_{n+1}=\frac{\varepsilon_\perp e^{i\gamma}}{\varepsilon-\varepsilon_0(n-f)^2+\varepsilon_{||}}u_n. \qquad (17.53)$$

The energy eigenvalues are

$$\varepsilon_n^{\pm}=\frac{1}{2}(\varepsilon_1+\varepsilon_2)\pm\frac{1}{2}\sqrt{(\varepsilon_1-\varepsilon_2)^2+4\varepsilon_\perp^2} \qquad (17.54)$$

where

$$\varepsilon_1=\varepsilon_0(n-f)^2+\varepsilon_{||},\quad \varepsilon_2=\varepsilon_0(n+1-f)^2-\varepsilon_{||}$$

The current in the ring is found by differentiating the energy with respect to the Aharonov-Bohm flux $\Phi$ (and putting the latter to zero if the *total* flux vanishes, due to possible compensation between the solenoid flux and the flux created by the Zeeman field, $B_z$)

$$J=-\frac{e}{h}\sum_{n=-\infty}^{\infty}\sum_{\sigma=-1}^{1}\left\{\exp\left[\frac{\varepsilon_{n\sigma}(f)-\zeta}{T}\right]+1\right\}^{-1}\frac{\partial}{\partial f}\varepsilon_{n\sigma}(f)\,. \qquad (17.55)$$

Expression (17.55) can be easily evaluated. Skipping the corresponding lengthy formula, we show below the representative dependences of the persistent currents on the longitudinal flux $\Phi$ and on the tilt angle $\alpha$ between the perpendicular field $B_\perp=\sqrt{b_r^2+B_\varphi^2}$ and the Zeeman field $B_{||}$.

Fig. 17.8 shows the current as a function of flux in the ring $\Phi$ in case when the ratio of the Zeeman energy $\varepsilon_Z$ to the distance between the discrete energy levels at the Fermi energy $\Delta E=2n_F\varepsilon_0$ equals to 5.

$\Delta E$ is the representative energy scale for the Aharonov-Bohm effect whereas the projections of $\varepsilon_Z$ to the ring plane and on the symmetry axis determine the spin-related Berry-phase energy scales $\varepsilon_\perp$, $\varepsilon_{||}$. In case when $\alpha=0$ or $\alpha=\pi/2$, the current vanishes at zero Aharonov-Bohm flux, as was mentioned in [13]. Persistent current is an oscillating function of the Aharonov-Bohm flux at any value of $\alpha$, it does not depend on the angle $\gamma$ between the azimuthal and radial field components. The shift of position of the minima in $J(f)$ dependences is in accord with the expected Berry phase shift from Eq. (17.46)

$$\Delta f=\frac{1}{2}\sin\alpha. \qquad (17.56)$$

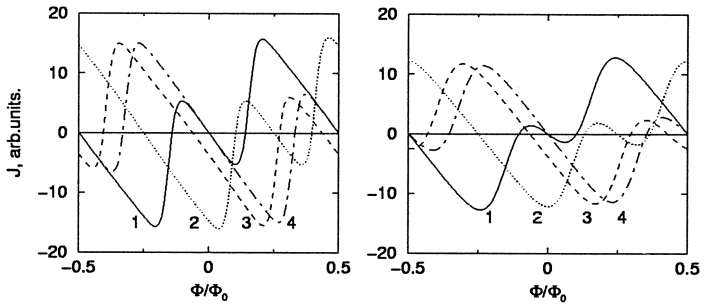


*Figure 17.8* Aharonov-Bohm current versus magnetic flux at various values of the Berry angle $\alpha$ and the temperature $\tau$. Left panel: $\tau = 0.02$, right panel: $\tau = 0.05$. Line 1 in both panels corresponds to $\alpha = 0$, line 2 to $\alpha = \pi/6$, line 3 to $\alpha = \pi/3$ and line 4 to $\alpha = \pi/2$. Electron concentration is chosen according to the value of parameter $n_F = 10.25$.

There remains a mystery on the origin of persistent current at $f = 0$, in particular this current shows the non-monotonic dependence on temperature with a maximum at low temperature.

Fig. 17.9 shows the dependence of the persistent current on $\varepsilon_\perp$ at fixed longitudinal flux. The oscillation displayed are the manifestation of an another effect, similar to the De Haas-Van Alphen effects in metals, and can be accounted for by the passage by the Zeeman-split Fermi energy through the set of quantized energy states in a ring in the vicinity of the Fermi energy. Since the energy of the states depends on $\Phi$, persistent current is also an oscillating function of $\Phi$ with a period $\Phi_0$.

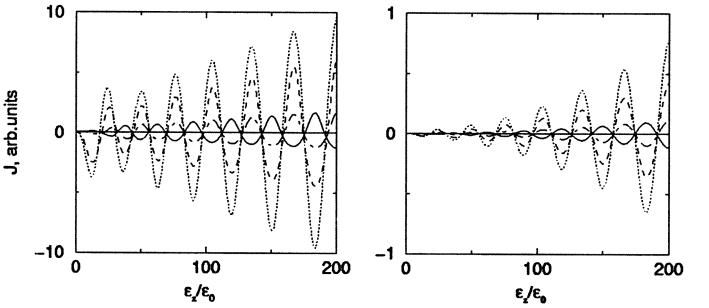


*Figure 17.9* Aharonov-Bohm current versus the Zeeman splitting $\varepsilon_Z$ at temperature $\tau = 0.2$ (left panel) and $\tau = 0.5$ (right panel). In both panels, solid line corresponds to $\alpha = 0$, dotted line to $\alpha = \pi/6$, dashed line to $\alpha = \pi/3$ and dot-dashed line to $\alpha = \pi/2$. Parameter $n_F = 10.25$.

## 7. EXOTIC AHARONOV-BOHM AND BERRY-PHASE EFFECTS

The understanding of phase coherence in mesoscopic specimens stimulated search for various generalizations of the generic situation depicted with the Aharonov-Bohm phase. We mention some of those within the limits of our competence.

The phase shift of the electron wave function can be produced by spin-orbit interaction [35]

$$H_{so} = -\frac{\hbar}{4m^2c^2}\vec{\sigma}\cdot(\mathbf{p}\times\nabla)V(\mathbf{r}) = \frac{\hbar^2}{4m^2c^2}\left(\frac{1}{r}\frac{dV}{dr}\right)1\cdot\vec{\sigma} \qquad (17.57)$$

where $V(\mathbf{r})$ is an electrostatic potential. In case when $V$ is created by a charged line with a linear charge density $\tau$ inserted into the ring (Fig. 17.10a), the phase shift (known as the Aharonov-Casher effect [36]) becomes

$$\delta = \frac{e\tau}{mc^2}(n_\uparrow - n_\downarrow). \qquad (17.58)$$

The interaction Hamiltonian describing this effect, to be added to the Hamiltonian in Eq. (17.48), is

$$H_{int} = -\frac{ie\hbar^2\tau}{2m^2c^2R^2}\sigma_z\frac{\partial}{\partial\varphi}. \qquad (17.59)$$

The phase shift is very small a compared to the Aharonov-Bohm shift $(\Delta\varphi)_{AB}$,

$$\delta/(\Delta\varphi)_{AB} \sim \frac{V}{mc^2}\times\frac{g\mu_B}{\varepsilon_F}. \qquad (17.60)$$

Even for the semiconducting crystals with a large g-factors [37], $\delta$ remains much smaller than $(\Delta\varphi)_{AB}$.

For the atomic potentials of randomly distributed spins, according to [38], Aharonov-Bohm persistent current shifts in phase as

$$J = \frac{1}{2}[J_{AB}(2\pi\Phi/\Phi_0 + \delta) + J_{AB}(2\pi\Phi/\Phi_0 - \delta)]. \qquad (17.61)$$

Similar spin-orbit effects have been considered by a number of authors [39], *etc.* The Aharonov-Casher effect has been suggested for neutral particles such as atoms in liquid helium [40].

It was proposed [41, 42] and possibly, found in an experiment [43], that persistent current may exist in the nonmetallic materials such as Peierls insulators.

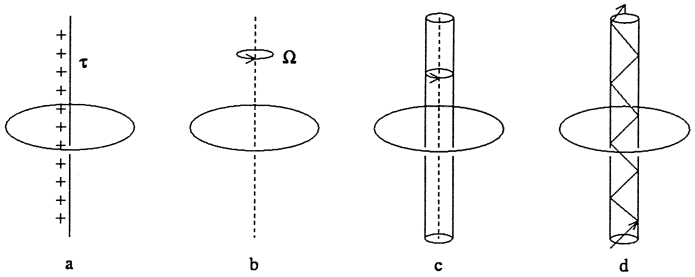


*Figure 17.10* Possible geometrical and topological Aharonov-Bohm configurations: (a) Ring pierced by a charged dielectric line (Aharonov-Casher geometry); (b) Rotating ring; (c) Ring in the Lense-Thirring field of a rotating massive body; (d) Ring enclosing an optical fiber transmitting the electromagnetic radiation through its orifice.

Geometrical phase may appear in a rotating metal (Fig. 17.10*b*), and even cause "persistent rotation" of the latter in the Aharonov-Bohm field [44]. This is extremely weak effect requiring, for its observation, temperatures in the range of $\mu$K even in nanoscopic samples ($R \leq 10^{-6}$ cm). Even smaller are the effects of gravitational interaction with the rotating massive bodies (Fig. 17.10*c*) producing the Lense-Thirring field [45] which results in the phase shift

$$\alpha \sim \frac{GmMR^2}{\hbar c^2}\Omega$$

where $G$ is gravitational constant, $R$ is radius and $M$ the mass (per unit length) of a cylinder rotating with an angular velocity $\Omega$. The latter effect is certainly out of reach to any terrestrial experiment.

The effects of time-dependent fluxes (Fig. 17.10*d*) have been considered by Aronov *et al.* [46] and by the author and Shumovsky [47]. The specific case of the so-called 2nd Aharonov-Bohm effect (the phase shift due to scalar potential) have been addressed in [13] and nominated as the "persistent charge", *i.e.*, periodic in the $VT$ charge accumulation on plates of a mesoscopic capacitor subject to voltage pulses of amplitude $V$ and duration $T$. A specific effect of inelastic backscattering in a "clean" ring is shown to restore the Aharonov-Bohm oscillation otherwise suppressed by a time varying magnetic flux [48, 49].

Strong coupling effects (Wigner crystallization [50]), Luttinger liquid [51]) make change to the amplitude of persistent current and its temperature dependence, in comparison to noninteracting electrons.

We mention also earlier works on flux quantization in bulk mesoscopic cylinders [52, 53, 54]. Due to surface electron states accumulating the Aharonov-Bohm phase in the same way as the rotating electrons in a

hollow cylinder do, magnetic moment of cylinder have been shown to oscillate in function of flux [52]. The oscillations are also seen in the longitudinal conductivity of Bi cylinders [53, 54]. These experiments have been the first demonstration of the quantum oscillations in mesoscopic specimens with the period of a single flux quantum $hc/e$.

## References

[1] E. Teller, Der diamagnetismus von freien electronen, Zs. Physik **67**, 311 (1931).

[2] L. D. Landau, Zs. Physik **64**, 629 (1930).

[3] Y. Aharonov and D. Bohm, Phys. Rev. **115**, 485 (1959).

[4] N. Byers and C. N. Yang, Theoretical considerations concerning quantized magnetic flux in superconducting cylinders, Phys. Rev. Lett. **7**, 46 (1961).

[5] F. Bloch, Flux quantization and dimensionality, Phys. Rev. **166**, 415 (1968);
Off-diagonal long-range order and persistent currents in a hollow cylinder, Phys. Rev. **137**, A787 (1965).

[6] I. O. Kulik, Flux quantization in a normal metal, JETP Lett. **11**, 275 (1970).

[7] M. Buttiker, Y. Imry and R. Landauer, Josephson behavior in small normal one-dimensional ring, Phys. Lett. **A96**, 365 (1983).

[8] M. V. Berry, Quantal phase factors accompanying adiabatic changes, Proc. Roy. Soc. (London) **A392**, 45 (1984).

[9] S. Washburn, Aharonov-Bohm effects in loops of gold, in: Mesoscopic Phenomena in Solids, *eds.* B. L. Altshuler, P. A. Lee and R. A. Webb, (Elsevier, 1991) p.1.

[10] Y. Imry, Physics of mesoscopic systems, in: Directions in Condensed Matter Physics, *eds.* G. Grinstein and G. Mazenko, (World Scientific, Singapore, 1986) p.101.

[11] S. Washburn and R. A. Webb, Aharonov-Bohm effect in normal metal. Quantum coherence and transport. Adv. Phys. **35**, 375 (1986).

[12] Y. Imry, Introduction to Mesoscopic Physics, (Oxford Univ. Press, Oxford, 1997).

[13] I. O. Kulik, Magnetic and electric Aharonov-Bohm effects in nanostructures, Physica B, **218**, 252 (1996).

[14] I. O. Kulik, Persistent current and persistent charge in nanostructures, in: Quantum Optics and Spectroscopy of Solids, *eds.* T.

Hakioglu and A. S. Shumovsky, (Kluwer Acad. Publ., Dordrecht, 1997) p.45.

[15] I. V. Krive and A. S. Rozhavsky, Non-traditional Aharonov-Bohm effects in condensed matter, Int. J. Mod. Phys. **B6**, 1255 (1992).

[16] D. Shönberg, Magnetic Oscillations in Metals, (Cambridge Univ. Press, Cambridge, 1984).

[17] J. M. Ziman, Principles of the Theory of Solids, (Cambridge Univ. Press, Cambridge, 1972).

[18] A. F. Andreev, Sov. Phys. JETP **19**, 1228 (1964); **22**, 455 (1966).

[19] I. O. Kulik, Macroscopic quantization and the proximity effect in *SNS* junctions, Zh. Eksp. Teor. Fiz. **57**, 1745 (1969) [Sov. Phys. JETP **30**, 944 (1969)].

[20] A. A. Abrikosov, Fundamentals of the Theory of Metals, (North-Holland, Amsterdam, 1988).

[21] R. Landauer, Electrical resistance of disordered one-dimensional lattices, Phil Mag. **21**, 863 (1970).

[22] H. F. Cheung, E. K. Riedel and Y. Gefen, Persistent current in mesoscopic rings and cylinders, Phys. Rev. Lett. **62**, 587 (1989).

[23] V. Chandrasekhar, R. A. Webb, M. J. Brady, M. B. Ketchen, W. J. Gallagher and A. Kleinsasser, Magnetic response of a single, isolated gold loop, Phys. Rev. Lett. **67**, 3578 (1991).

[24] D. Mally, C. Chapelier and A. Benoit, Experimental observation of persistent current in a GaAs-AlGaAs single loop, Phys. Rev. Lett. **70**, 2020 (1993).

[25] L. P. Levy, G. Dolan, J. Dunsmuir and H. Bouchiat, Magnetization of mesoscopic copper rings: Evidence for persistent currents, Phys. Rev. Lett. **64**, 2074 (1990).

[26] B. L. Altshuler, A. G. Aronov and B. Z. Spivak, JETP Lett. **33**, 94 (1981).

[27] D. Yu. Sharvin and Yu. V. Sharvin, JETP Lett. **34**, 272 (1982).

[28] B. L. Altshuler and A. G. Aronov, in: Electron-Electron Interactions in Disordered Systems, *eds.* A. L. Efros and M. Pollak, (Elsevier, Amsterdam, 1985) p.1.

[29] I. O. Kulik, "Transverse" persistent currents in mesoscopic cylinders and rings, To appear in Physica B, 2000.

[30] D. Eliahu, R. Berkovits, M.Abraham and Y. Avishai, Mesoscopic persistent-current correlations in the presence of strong magnetic fields, Phys. Rev. **B49**, 14448 (1994).

[31] C. A. Mead, The geometric phases in molecular systems, Rev. Mod. Phys. **64**, 51 (1992).

[32] L. D. Landau and E. M. Lifshitz, Quantum Mechanics, (Pergamon, New York, 1965).

[33] A. Stern, Berry's phase, motive forces, and mesoscopic conductivity, Phys. Rev. Lett. **68**, 1022 (1992).

[34] D. Loss, P. Goldbart and A. V. Balatsky, Berry's phase and persistent charge and spin currents in textured mesoscopic rings, Phys. Rev. Lett. **65**, 1655 (1990).

[35] R. Shankar, Principles of Quantum Mechanics, Plenum, New York, 1987.

[36] Y. Aharonov and A. Casher, Topological quantum effects for neutral particles, Phys. Rev. Lett. **53**, 319 (1984).

[37] E. N. Bogachek and U. Landman, Aharonov-Bohm and Aharonov-Casher tunneling effects and edge states in double-barrier structures, Phys. Rev. **B50**, 2678 (1994).

[38] Y. Meir, Y. Gefen and O. Entin-Wohlman, Universal effects of spin-orbit scattering in mesoscopic systems, Phys. Rev. Lett. **63**, 798 (1989).

[39] Y. Lyanda-Geller, Quantum interference and electron-electron interactions at strong spin-orbit coupling in disordered systems, Phys. Rev. Lett. **80**, 4273 (1998).

[40] A. V. Balatsky and B. L. Altshuler, Persistent spin and mass currents and Aharonov-Casher effect, Phys. Rev. Lett. **70**, 1678 (1993).

[41] I. O. Kulik, A. S. Rozhavsky and E. N. Bogachek, Magnetic flux quantization in dielectrics, Zh. Eksp. Teor. Fiz. Pis'ma **47**, 251 (1988) [JETP Lett. **47**, 304 (1988)].

[42] E. N. Bogachek, I. V. Krive, I. O. Kulik and A. S. Rozhavsky, Instanton Aharonov-Bohm effect and macroscopic quantum coherence in charge-density-wave systems, Phys. Rev. B42, 7614 (1990).

[43] Yu. I. Latyshev. O. Laborde, P. Monceau and S. Klaumunzer, Aharonov-Bohm effect on charge density wave (CDW) moving through columnar defects in $NbSe_3$, Phys. Rev. Lett. **78**, 919 (1997).

[44] I. O. Kulik, Small rigid rotators as qubits, in: Quantum Mesoscopic Phenomena and Mesoscopic Devices in Microelectronics, Program and Abstracts, p.108, *eds.* I. O. Kulik, R. Ellialtıoğlu, B. Tanatar and C. Yalabık., Bilkent Univ., Ankara, 1999.

[45] L. D. Landau and E. M. Lifshitz, Theory of Fields, (North-Holland, Amsterdam, 1988).

[46] I. E. Aronov, A. Grincwajg, M. Jonson, R. I. Shekhter and E. N. Bogachek, Sol. St. Communs. **91**, 75 (1994).

[47] I. O. Kulik and A. S. Shumovsky, Aharonov-Bohm effect induced by light in a fiber, Appl. Phys. Lett. **69**, 2779 (1996).

[48] T. Swahn, E. N. Bogachek, Yu. M. Galperin, M. Jonson and R. I. Shekhter, Phys. Rev. Lett. **73** 162 (1994).

[49] E. N. Bogachek, Yu. M. Galperin, M. Jonson, R. I. Shekhter and T. Swahn, J. Phys.: Cond. Matter **8**, 2603 (1996).

[50] I. V. Krive, P. Sandström, R. I. Shekhter, S. M. Girvin and M. Jonson, Phys. Rev. B **52**, 16451 (1995).

[51] M. V. Moskalets, Physica E **5**, 124 (1999).

[52] E. N. Bogachek and G. A. Gogadze, Sov. Phys. JETP **36**, 973 (1973).

[53] N. B. Brandt, D. V. Gitsu, A. A. Nikolaeva and Ya. G. Ponomarev, JETP Lett. **24**, 272 (1976).

[54] N. B. Brandt, E. N. Bogachek, D. V. Gitsu, G. A. Gogadze, I. O. Kulik, A. A. Nikolaeva and Ya. G. Ponomarev, Flux quantization effects in metal microcylinders in a tilted magnetic field, Fiz. Nizk. Temp. **8**, 718 (1982) [Sov. J. Low Temp. Phys. **8**, 358 (1982)].